



AIAA 2003-1725

**Computational Aeroelasticity:
Success, Progress, Challenge
(Invited)**

David M. Schuster
NASA Langley Research Center
Hampton, VA

Danny D. Liu
ZONA Technology
Scottsdale, AZ

Lawrence J. Huttzell
Air Force Research Laboratory
Wright-Patterson AFB, OH

AIAA Dynamics Specialists Conference
7 – 10 April 2003
Norfolk, VA

Computational Aeroelasticity: Success, Progress, Challenge

David M. Schuster^{*}
NASA Langley Research Center, Hampton, VA 23681

Danny D. Liu[†]
Arizona State University, Tempe, AZ 85287

Lawrence J. Huttzell[‡]
Air Force Research Laboratory, Wright-Patterson AFB, OH 45433

Abstract

The formal term Computational Aeroelasticity (CAE) has only been recently adopted to describe aeroelastic analysis methods coupling high-level computational fluid dynamics codes with structural dynamics techniques. However, the general field of aeroelastic computations has enjoyed a rich history of development and application since the first hand-calculations performed in the mid 1930's. This paper portrays a much broader definition of Computational Aeroelasticity; one that encompasses all levels of aeroelastic computation from the simplest linear aerodynamic modeling to the highest levels of viscous unsteady aerodynamics, from the most basic linear beam structural models to state-of-the-art Finite Element Model (FEM) structural analysis. This paper is not written as a comprehensive history of CAE, but rather serves to review the development and application of aeroelastic analysis methods. It describes techniques and example applications that are viewed as relatively mature and accepted, the "successes" of CAE. Cases where CAE has been successfully applied to unique or emerging problems, but the resulting techniques have proven to be one-of-a-kind analyses or areas where the techniques have yet to evolve into a routinely applied methodology are covered as "progress" in CAE. Finally the true value of this paper is rooted in the description of problems where CAE falls short in its ability to provide relevant tools for industry, the so-called "challenges" to CAE.

INTRODUCTION

Nearly 70 years ago, Theodorsen¹ published a now famous report outlining, in detail, an analytical method by which the flutter characteristics of airfoils with two or three degrees-of-freedom could be theoretically calculated. This development laid the

^{*} Senior Research Engineer, Associate Fellow AIAA.

[†] Professor, Fellow AIAA.

[‡] Senior Aerospace Engineer, Associate Fellow AIAA.

Copyright © 2003 by the American Institute of Aeronautics and Astronautics, Inc. No copyright is asserted in the United States under Title 17, U.S. Code. The U.S. Government has a royalty-free license to exercise all rights under the copyright claimed herein for Governmental Purposes. All other rights are reserved by the copyright owner.

groundwork for what has become a rich area of research in theoretical aeroelasticity.

Recently, the term Computational Aeroelasticity (CAE) has been coined, and the term generally is used to refer to the coupling of high-level Computational Fluid Dynamics (CFD) methods to structural dynamics tools to perform aeroelastic analysis. However, given the large body of research that has led us to this point, it is inappropriate to constrain the definition of CAE in this fashion.

This paper asserts a much broader definition of the term, one in which CAE encompasses all levels of aeroelastic analysis. Aeroelastic tools based on both linear unsteady aerodynamics and nonlinear CFD methods have been developed and successfully applied. We refer to both of these methodologies as components of CAE. Likewise structural modeling as simple as beam theory to state-of-the-art Finite Element Modeling (FEM) have been incorporated

into aeroelastic tools and these techniques should also be included under the CAE heading.

It is not the intention of this paper to provide an exhaustive history of the development and application of CAE over the past 70 years. Rather, the subject will be examined in the context of two primary themes:

- 1) Aeroelastic problems requiring theoretical investigation;
- 2) Strategies and techniques attacking these problems.

The discussion will be broken into three distinct categories. Problems that are relatively well understood and associated CAE tools that are viewed as mature and accepted for these types of problems will be discussed as the “successes” of CAE. Emerging, less understood aeroelastic problems where CAE has been applied on a limited basis, or a one-of-a-kind application of CAE, will be examined as “progress” in CAE. Finally, problems which continue to contest CAE methodology and roadblocks to the future development and application of CAE will be discussed as the “challenges” to CAE.

This categorization provides a reasonable roadmap for the future development of CAE. The “successes” provide us with a template for future development. They represent the tools that the user community is willing to employ on a day-to-day basis, and the problems that are important to the development of current aerospace vehicles. The “progress” categorization illustrates the types of problems that are beginning to limit the development and/or performance of vehicles and analysis techniques that can be developed by stretching the current technology. The “challenge” categorization provides a target or focus for future development. Even with today’s advanced methodologies and computational capability, there are problems that cannot be accurately or efficiently modeled using current techniques, particularly in the area of nonlinear unsteady aerodynamics.

Each of these areas will be discussed in detail with specific examples illustrating the various assertions. Finally, our view of the grand challenge to the future development of CAE methodology will be outlined and discussed.

SUCCESSSES IN COMPUTATIONAL AEROELASTICITY

Despite the complexity of coupling three distinct engineering disciplines, aerodynamics, structures, and dynamics into a unified aeroelastic analysis capability, computational aeroelasticity has enjoyed a

significant number of successes over its course of development. Today, every manned vehicle that flies through our atmosphere undergoes some level of aeroelastic analysis before flight. Virtually every major unmanned flight vehicle is similarly analyzed.

Flutter is a catastrophic aeroelastic phenomenon that must be avoided at all costs, and all flight vehicles must be clear of flutter and many other aeroelastic phenomena in their flight envelope. Flight and wind-tunnel testing are two ways to clear a vehicle for flutter, but both are expensive and occur late in the design process. Therefore, engineers rely heavily on computational methods to assess the aeroelastic characteristics of flight vehicles. The successes of computational aeroelasticity are rooted in this aeroelastic characterization process.

Problem Formulation

When examining the subject of CAE, one cannot overlook the simple elegance of the formulation of the problem. The development of the generalized aeroelastic equations of motion is enabling for most modern CAE tools, and should be viewed as one of the true successes in CAE. The generalized aeroelastic equations of motion are given by:

$$[M]\{\ddot{q}(t)\} + [D]\{\dot{q}(t)\} + [K]\{q(t)\} = \{F(t)\} \quad (1)$$

$$\{w(x, y, z, t)\} = \sum_{i=1}^{N_{Modes}} q_i(t)\{\phi_i(x, y, z)\} \quad (2)$$

where $\{w(x, y, z, t)\}$ is the structural displacement at any position and time on the vehicle, and $\{q(t)\}$ is the so-called generalized displacement vector, both of which are simply geometric properties describing the time history of the aeroelastic deformation. $[M]$, $[D]$, and $[K]$ are the generalized mass, damping and stiffness matrices respectively, and ϕ_i represents the normal modes of the structure. These terms result purely from the structural and mass properties of the vehicle. The $\{F(t)\}$ term is the generalized force vector and represents the coupling of the unsteady aerodynamics and inertial loads with the structural dynamics. Thus the coupled aeroelastic equations of motion are comprised of distinct terms that can be related to the structures, aerodynamics, and dynamics disciplines that are required to formulate the problem. This allows great flexibility in the choice of methods that can be used to model a given system. For instance, for linear structural models, the generalized mass, damping and stiffness matrices are constants that do not vary with time or the structural deformation. This remains true independent of the aerodynamics chosen for representation of the generalized force. Thus the structural and aerodynamic models under this formulation remain completely independent of each other. Varying

levels of fidelity, sometimes termed “variable fidelity modeling,” of structural and aerodynamic modeling can be readily matched to the problem under analysis without changing the overall formulation of the equations of motion.

This mix and match characteristic is exploited quite regularly through the choice of the unsteady aerodynamic simulation used to construct the generalized force term. This term has been modeled using aerodynamics methods that range from linear doublet lattice and kernel function solutions in the frequency domain to solution of the three-dimensional unsteady Reynolds Averaged Navier-Stokes equations in the time domain. When both the structures and aerodynamics are linear, solution of the generalized aeroelastic equations of motion reduces to computation of the complex Eigenvalues of the stability matrix, whose values determine the stability of the system. Computations involving nonlinear aerodynamics and/or structures are typically performed in the time domain, which tend to complicate the process of determining system stability, but nevertheless stem from the same formulation of the problem.

This unique formulation of the equations of motion also facilitates the systematic evaluation of an aeroelastic system. Virtually all aeroelastic analyses begin with an analysis of the system stability that involves the use of linear structural and aerodynamic models. As critical points in the aircraft design and/or flight envelope are identified, the analysis can be, and regularly is, refined through incorporation of higher fidelity structural or aerodynamic models, as appropriate. This approach to the analysis provides the designers with an improved confidence that the design will be free from aeroelastic anomalies throughout the flight envelope. In addition, the approach provides designers with important data regarding the sensitivity of the design to nonlinear effects.

Subsonic/Supersonic Aeroelastic Analysis of General Aircraft Configurations

Linear subsonic and supersonic aeroelastic analysis of general aircraft configurations has matured over the last 20 years, and these types of computations are performed routinely today. Tools are now commercially available which allow aeroelastic modeling and analysis to be performed directly from existing structural Finite Element Models (FEM). Trimmed static aeroelasticity, flutter, divergence, gust response, and aeroservoelastic response are among the simulations that can be readily computed using these tools.

Linear analyses typically involve modeling complex systems with either simplified geometric or physical properties. In the case of linear aeroelastic analysis, the physics of the problem are modeled at a lower fidelity so that the problem can be linearized. Geometric approximations are usually introduced into the aeroelastic models as well, but in general, these methods are capable of modeling relatively complete, geometrically complex configurations. The majority of modern linear aeroelastic methods are highly developed tools that provide the user with a broad range of functionality and analysis options. The methods are computationally efficient, making them expedient as rapid analysis and Multidisciplinary Design and Optimization (MDO) tools. They also have the desirable property that classical problems with exact solutions can usually be easily modeled, significantly simplifying the verification tasks for newly developed methods.

Two types of linear aeroelastic analysis will be highlighted here. The first describes examples of linear flutter analysis using these techniques. The second discusses linear aeroservoelastic and gust response simulations.

Linear Flutter Analysis

An example flutter analysis of the X-43A research and launch vehicle is described in Figure 1. In this case the complete X-43A hypersonic research and launch vehicles were modeled structurally using FEM techniques. The model for this portion of the analysis is shown in the upper left portion of the figure. A normal modes structural dynamics analysis was performed to obtain rigid body and structurally flexible mode shapes and frequencies as depicted in the lower left portion of the figure. The model for the unsteady aerodynamics portion of the analysis is shown in the upper right corner. For this analysis, doublet lattice² aerodynamics was used in the subsonic flight regime, while the ZONA51³ linear unsteady aerodynamics methodology was used in the supersonic regime.

Mode shapes from the structural dynamics analysis are interpolated onto the aerodynamics grid using a surface splining technique⁴. This allows the generalized aerodynamic force term of Equation (1) to be computed directly from the unsteady aerodynamic analysis. Finally, the resulting flutter analysis obtained at a fixed Mach number is depicted in the lower right corner. This figure outlines the general procedure used for most of today’s linear flutter and aeroelastic analyses. There are a number of proprietary and off-the-shelf packages available to perform this type of analysis, and the choice of

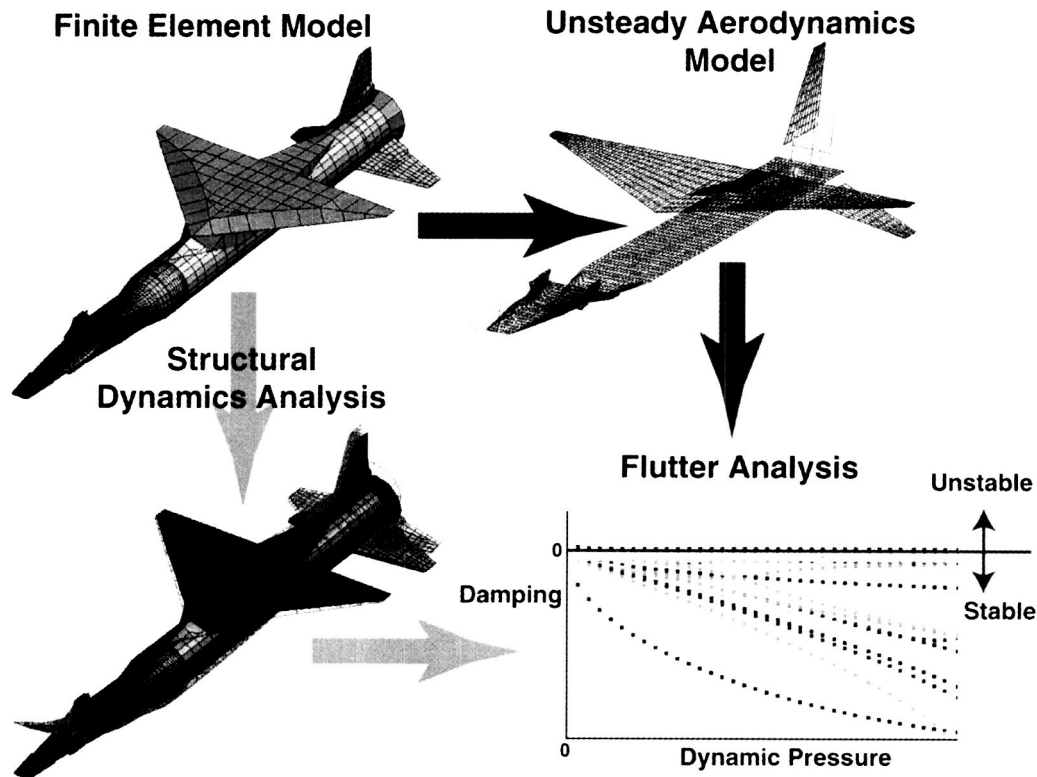


Figure 1. X-43A Flutter Analysis.

method is primarily one of user preference. Thus, linear flutter analysis is substantially viewed as a mature science.

To further emphasize the broad range of functionality available in these methods, a second example describing the aeroelastic analysis of three F-16 configurations, each with different store combinations, is shown in Figure 2. Chen et al.⁵ use a modified form of the ZAERO⁶ aeroelastic method to compute the flutter and Limit Cycle Oscillation (LCO) characteristics of this aircraft. In the transonic speed regime the classical linear aerodynamics are replaced by time-linearized transonic aerodynamics based on a nonlinear aerodynamic analysis of the mean flow about the aircraft. This option, known as ZTAIC, allows steady flow nonlinearity in the transonic flight regime to be introduced into the analysis, without sacrificing the attractive linear efficiency of ZAERO. ZTAIC uses nonlinear steady pressures as input to the analysis to introduce the steady nonlinearity. It is postulated that this nonlinearity may be sufficient to capture some LCOs. Some features of three aeroelastic phenomena, as described by Denegri⁷, were computed in this

analysis: classical flutter, typical LCO, and non-typical LCO.

While there remains considerable debate over the nonlinear mechanisms resulting in LCO, particularly on the F-16 aircraft, these analyses are an excellent example of how existing linear methods are being continuously modified and extended to attack problems of interest to the aerospace community.

An important byproduct of this and the following aeroservoelastic examples is the development of a new flutter solution technique known as the g-method⁸. The g-method generalizes the conventional k- and p-k methods and provides more reliable damping for flutter predictions. The method yields an exact flutter equation solution accurate up to the first order of damping. This solution can be derived from the Laplace-domain aerodynamics and is valid throughout the entire reduced frequency domain. The g-method utilizes a reduced-frequency sweep technique to search for the roots of the flutter solution and a predictor-corrector scheme to ensure the robustness of the sweep technique. This solution algorithm has proven to be efficient and robust and can obtain large numbers of aerodynamic lag roots, as demonstrated by the cases of References 5 and 8.

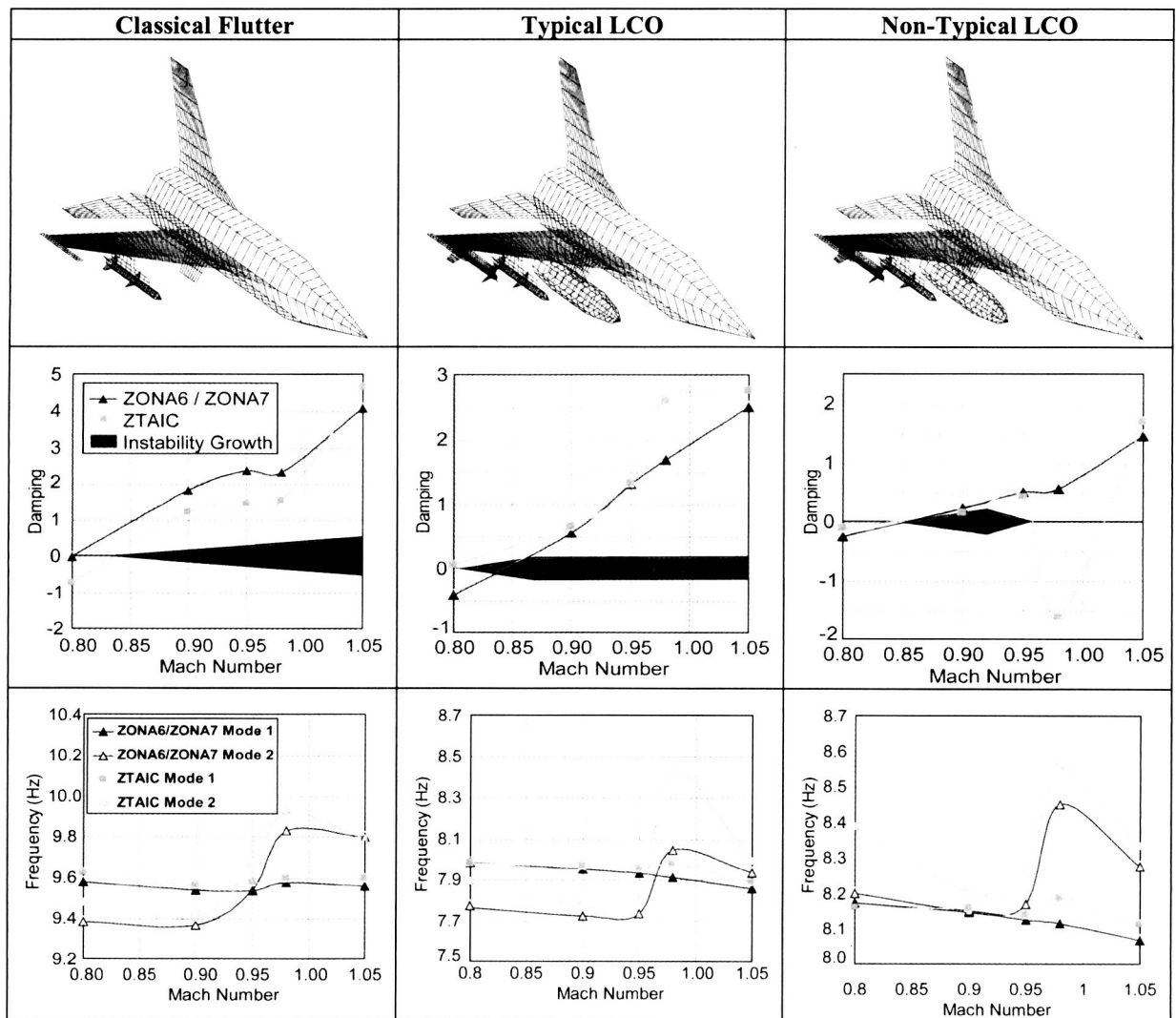


Figure 2. Transonic AIC (ZTAIC) versus classical linear aeroelastic analysis of flutter/LCO for an F-16 aircraft force with wing stores (Reference 5).

Karpel⁹ has recently extended this method to simulate aeroservoelastic problems in the frequency domain, providing a new complementary analysis technique to the s-domain simulations discussed below.

Linear Aeroservoelastic and Gust Response Analysis

Aeroservoelastic (ASE) and gust response analyses are also performed on a relatively regular basis using linear aeroelastic analysis methods. For these applications, external forcing terms are added to the generalized force term of Equation (1), a term describing the generalized force due to control deflection, and a term describing the generalized force due to a gust. The equations are typically solved in state-space form and are constructed from separate models of the aeroelastic system, the vehicle dynamics sensors, the control actuators, the control

system, and the gust spectrum. The generalized force terms are expressed as rational functions of Laplace variables in the s-domain. This is done, for example, using the classical Rogers approximation¹⁰ or the minimum-state method of Karpel¹¹, which is applied presently.

Two ASE examples are presented. The first demonstrates flutter suppression on an F-16 wing, and the second investigates gust response reduction for an F-18 aircraft¹². A modified version of the Automated Structural Optimization System¹³ (ASTROS) is used as an ASE analysis tool for both examples. The method, known as ASTROS*¹⁴, seamlessly interfaces with the ZAERO linear aerodynamic and aeroservoelastic modules.

Figure 3 shows the structural, aerodynamic, and controls models for the flutter suppression analysis of

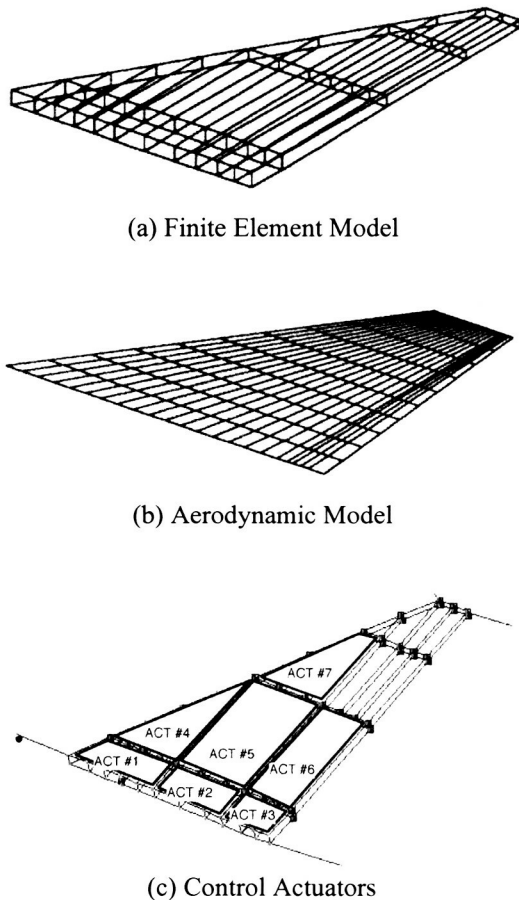


Figure 3. Finite element, aerodynamic, and control actuator models of an F-16 wing (Reference 12)

the F-16 wing. The control system for this flutter suppression system consists of seven piezoelectric (PZT) actuators, as shown in the figure. An active control system using the PZT actuators was designed to increase the open loop flutter speed by approximately 12%.

Both open and closed loop flutter analyses were performed using the ASTROS* methodology and results are summarized in Figure 4. At the design condition, the first and second modes of the open-loop system are unstable, as shown by the open square and triangle residing in the right-half plane in the figure. Under the closed-loop control, these two modes move to the left-half plane as designated by the solid symbols, thus stabilizing the system.

Figure 5 shows the modal displacement time histories for the open and closed loop systems after a perturbation of the system. The open-loop system is clearly divergent while the closed-loop system rapidly converges to a stable state.

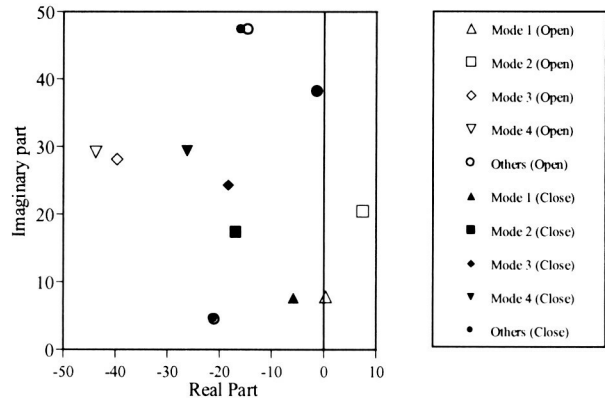
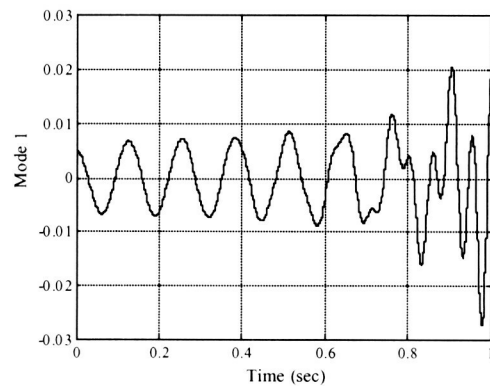
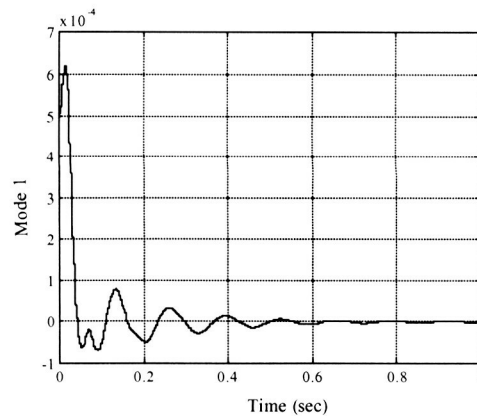


Figure 4. Open and Closed Loop Eigenvalues of the System at Design Airspeed, Mach=0.9 (Reference 12)



(a) Open Loop System



(b) Closed Loop System

Figure 5. Modal time histories for the open and closed loop flutter suppression system. (Reference 12)

Figure 6 shows the finite element and aerodynamic models of an F-18 aircraft¹⁵ that is used to design and analyze a gust response reduction system. This model has four control surfaces; inboard/outboard leading edge flaps, trailing edge flap and aileron. These

control surfaces are actuated to reduce the structural response of the aircraft to an atmospheric gust.

The ASTROS* open loop flutter analysis results in a flutter driven by the wing's torsion mode at an airspeed of 636 ft/sec. The gust response reduction active control system is tailored at the design airspeed of 500 ft/sec, which is 78% of the open loop flutter speed. Figure 7 shows the RMS values of the second structural mode, the torsion mode, due to a gust over a range of airspeeds. For comparison, the RMS values of both open loop and closed loop systems are shown. The RMS values of the closed loop system are substantially reduced throughout the airspeeds of interest.

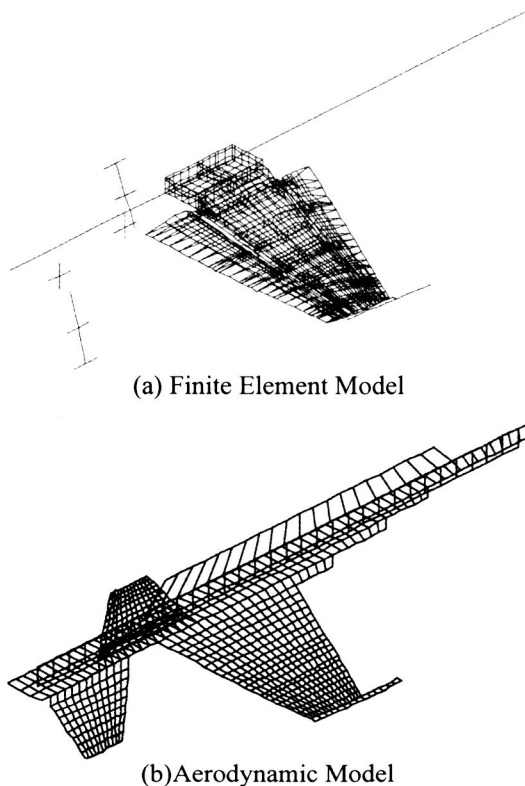


Figure 6. F-18 finite element and aerodynamic models for gust load alleviation analyses. (Reference 12)

Both of these examples demonstrate that relatively complex aeroservoelastic systems can be analyzed using state-of-the-art linear aeroelastic methodologies. Advanced control systems can be analyzed with and without aeroelastic effects to determine the sensitivity of the design to aeroelasticity. Gust response of aeroelastic systems can be assessed using these methods, and control systems to reduce this response can be readily evaluated. Flutter suppression control systems can be investigated and any number of aeroservoelastic phenomena can be analyzed using these techniques.

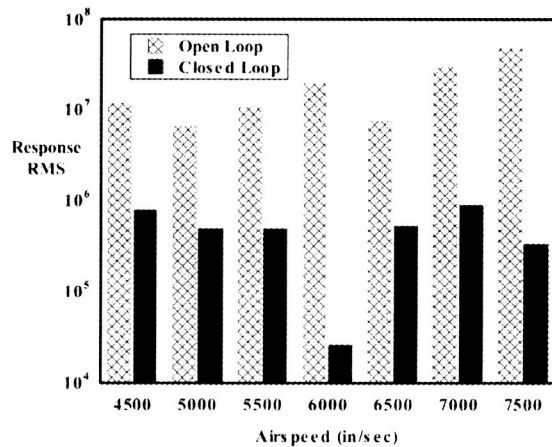


Figure 7. Root mean square values of modal response due to a gust versus airspeed. (Reference 12)

The methodology behind these analyses is among the most remarkable of the CAE success stories.

Transonic Wing Flutter

In the transonic speed range, aeroelastic analysis becomes significantly more complicated. Under these conditions, shock waves can form and disappear as the aircraft undergoes unsteady, structurally flexible motion. In addition, regions of separated flow can appear and disappear as these shock waves strengthen and weaken. These are highly nonlinear events that can have a profound impact on the aeroelastic behavior of flight vehicles. Using flutter as an example phenomenon, the impact of transonic unsteady aerodynamics on aeroelastic stability will be discussed.

The appearance of shock waves on the vehicle can cause a further drop in the flutter boundary in the transonic speed regime over that produced by linear compressible flow effects. This drop is termed the transonic dip. The important feature of the transonic dip is the bottom of the dip, which defines the minimum velocity at which flutter can occur across the flight envelope of the vehicle. Therefore, predicting the bottom of this dip is often crucial to the design of the vehicle.

Figure 8 presents an idealized flutter boundary through the transonic speed regime along with illustrations of typical computed results using various CAE methods. The solid line depicts the measured flutter boundary, and an expected result from a flutter analysis using linear unsteady aerodynamics is shown as the long-dashed line. As can be seen, the linear analysis typically predicts the flutter boundary adequately at subsonic and supersonic speeds, but is unconservative in the transonic speed regime where it

typically predicts a higher flutter dynamic pressure, and consequently velocity, than experiment. The flutter boundary predicted by a nonlinear, inviscid unsteady aerodynamics analysis is depicted by the dotted line. This analysis could be obtained by solving the unsteady transonic small disturbance potential flow, full potential flow, or Euler aerodynamic equations of motion. All of these methodologies have the capability of predicting shock waves in the flow, frequently resulting in a drop in the flutter boundary in the transonic speed regime. However, if viscous effects are not included in the analysis, the predicted boundary can often be over-conservative, predicting a significantly lower flutter speed at the bottom of the transonic dip. Viscous effects in the form of significant boundary layer thickening and/or shock-induced flow separation tend to define the bottom of the transonic dip, and it is only when these effects are added, as shown by the short-dashed line, that an accurate prediction of transonic flutter characteristics can be anticipated.

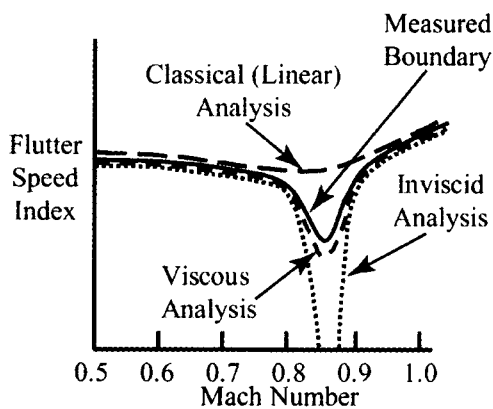


Figure 8. Idealized flutter boundary and CAE predictions.

The severity of the dip and its Mach number range are highly dependent on the aerodynamic characteristics of the vehicle to be analyzed. Modern transports employing supercritical wing technology can experience significant transonic effects due to large unsteady motion of the shock wave across the wing chord. Wings with weaker shocks or shocks whose position is not highly sensitive to changes in local angle of attack will not experience as drastic transonic effects. These characteristics are directly related to the wing sweep, thickness, and camber distribution. Thus the prediction of flutter characteristics in the transonic speed regime can be precarious since it is difficult, if not impossible, to predict when transonic effects will have a major impact on the flutter boundary.

The addition of nonlinearity and viscous effects to the unsteady aerodynamics analysis is not trivial. The nonlinearity of the problem typically forces the analyses to be performed in the time domain as opposed to the frequency domain for linear flows. Methods for determining the stability boundary using time domain aerodynamics are not as simple and require a significant amount of computation and user interfacing to determine the boundary. The addition of viscous effects further complicates the process by adding longer computation times and more uncertainty in the form of turbulence modeling. Therefore, the successes in transonic flutter prediction have been limited primarily to transonic wing flutter. Modeling and computational requirements for more complete configuration unsteady viscous analyses have limited the widespread development and application of these types of methods to anything but the simplest of geometries. However, the advances in the use of these methods for transonic aeroelastic analysis of wings are remarkable.

Two examples of this type of application that illustrate the problems with predicting transonic aeroelasticity are presented here. The first is a series of transonic wing flutter computations by Lee-Rausch and Batina¹⁶ using Euler and Navier-Stokes unsteady aerodynamics for the AGARD 445.6 wing. The CFL3DAE code¹⁷ was used for these computations. The planform for this wing and a summary of the flutter analysis using Euler and Navier-Stokes unsteady aerodynamics is shown in Figure 9. The AGARD 445.6 wing has a quarter-chord sweep of 45°, and a symmetrical airfoil with a maximum thickness of 4%. While there is an appreciable transonic dip for this wing, as tested in air, flutter computations using the Euler equations were able to predict the bottom of the flutter dip in the transonic speed regime, and addition of viscous effects to the analysis did not show an appreciable change in the results. The thin airfoil profile and high wing sweep combine to minimize transonic effects on this wing, resulting in this benign flutter behavior in the transonic range. At the low supersonic Mach numbers however, the Euler equation analysis predicted a significantly higher flutter boundary, and addition of viscous effects through solution of the RANS equations improved the simulation considerably.

Gibbons¹⁸ demonstrated a somewhat different result in his analysis of the transonic flutter characteristics of a business jet wing using the CAP-TSD²⁰ and CFL3DAE aeroelastic methods. The wing planform and flutter results from this analysis are summarized in Figure 10. In contrast to the AGARD 445.6 wing, this wing has a quarter-chord sweep of approximately

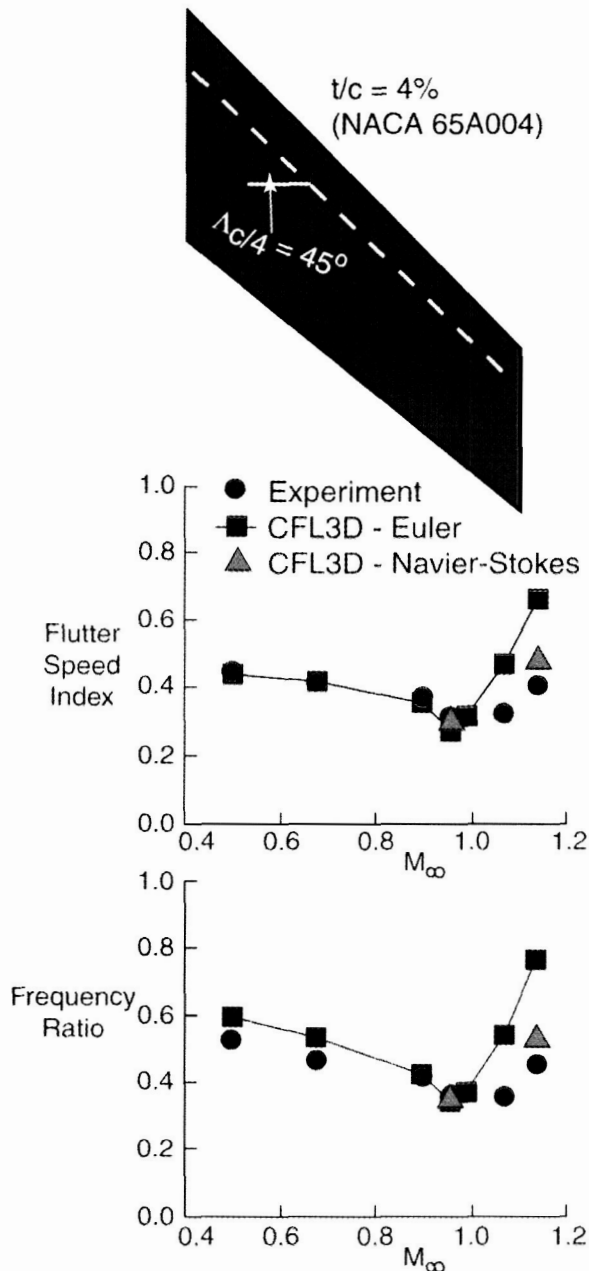


Figure 9. AGARD 445.6 flutter computations using Euler and Navier-Stokes unsteady aerodynamics (Reference 16).

27° , and the airfoil thickness varies from 13% at the wing root to 8.5% at the wing tip. The flutter boundary shown in the figure is plotted as flutter speed index versus Mach number. Results from two inviscid analyses and a viscous analysis are compared with wind tunnel data. For both inviscid cases, the calculated flutter boundary drops off rapidly as Mach number increases into the transonic regime. The faired line in the figure represents the CFL3D Euler computations. At Mach 0.90, the Euler computations

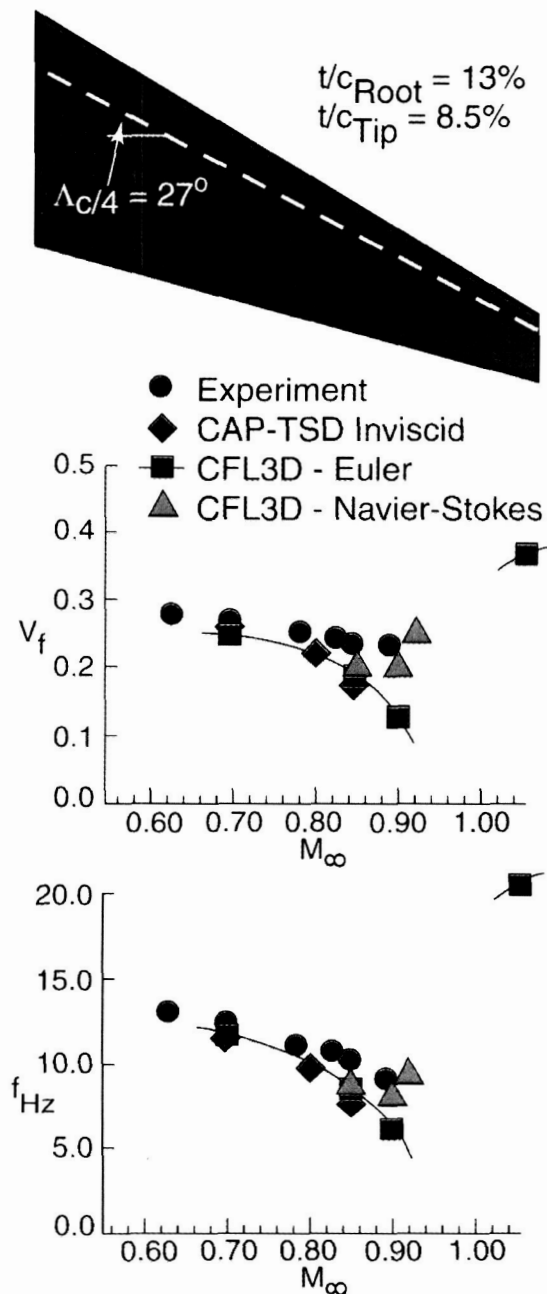


Figure 10. Inviscid and viscous flutter calculations on a business jet wing. (Reference 18)

contained enough aerodynamic damping to identify the flutter boundary shown by the square symbol. However, at this Mach number, the inviscid CAP-TSD result indicated a free response with no appreciable aerodynamic damping even for very low dynamic pressures. Euler calculations were performed at Mach 0.92 and 0.94, and showed a similar free-response characteristic. Thus the inviscid transonic methodologies employed on this wing predict a flutter boundary that dips to very low,

unrealistic velocities at transonic speeds. The addition of the viscous terms in the CFL3D computations, with appropriate changes to the wing grid, raises the predicted Mach 0.92 and 0.94 flutter boundaries to the level indicated by the triangle symbols in the figure. These viscous results are in much improved agreement with the behavior observed in the wind tunnel. Similar improved agreement has been obtained with a viscous version of the CAP-TSD transonic small disturbance potential flow code.¹⁹

While there is data that indicates that nonlinear inviscid analysis methods may be capable of predicting the transonic dip in isolated flutter cases, it would certainly seem prudent to include viscous effects in all transonic flutter analyses. It appears that nonlinear inviscid methods produce results that are conservative in the transonic speed regime, but this has not been definitively proven. Flutter margin is often a critical parameter in aircraft design, and overly conservative flutter margins can often result in unnecessary added structural weight and/or reduced vehicle performance.

The results discussed here, are enlightening from a research and phenomenological understanding standpoint, and certainly demonstrate the high-quality results that can be obtained when using high-order viscous unsteady aerodynamics. However, these applications are for wing-alone geometries, and have limited value in vehicle design application, where the interaction of complex geometric components can have a first order effect on the aeroelastic performance of the vehicle. So while these applications are viewed as a success, they also highlight one of the chief roadblocks to application of higher-order unsteady aerodynamics methods to aeroelastic problems. The human and computational resources required to apply these methods to problems of higher complexity than individual vehicle components precludes them from being used more extensively in general aeroelastic analysis.

PROGRESS IN COMPUTATIONAL AEROELASTICITY

The previously discussed successes of CAE have led to a number of isolated investigations and applications that tend to use the available CAE technology in innovative or novel ways, but have not yet received the attention to elevate the capability to mainstream application or research. This section highlights a few of these areas and discusses their role in current and future CAE development.

In general, the applications discussed here tend to stretch the available technology beyond the current accepted limits of application. In doing so, they

highlight the shortcomings of the current technology, and provide direction for future, more generalized development. In short, they represent the breeding ground for future CAE research and development.

Nonlinear Aeroservoelastic Analysis

CAE methods have been applied to a number of problems involving aeroservo and aeroservoelastic analyses. CAE methods involving linear aerodynamics can be applied to some problems in this area as long as the control surface deflections are small, and the geometrical discontinuities generated by activation of the control system do not generate aerodynamic nonlinearities in and of themselves. Unfortunately for most realistic control surface deflections, this is not the case and separated flows in the vicinity of hinge lines and near control surface edges quickly degrade the accuracy of linear aerodynamic analyses. To combat these problems, researchers have applied various levels of nonlinear unsteady aerodynamic analysis methods to the prediction of unsteady airloads due to control surface deflection. Two notable examples of this type of analysis are presented here.

B-2 Residual Pitch Oscillation

During flight-testing of the B-2 bomber, a nonlinear aeroelastic Residual Pitch Oscillation (RPO) was encountered after control surface pitch doublets were input at conditions outside the aircraft's flight envelope²¹. The initial vehicle response to the control surface doublet decayed in amplitude to a small limit cycle RPO after several pitch cycles. Video from a chase plane showed a moving shock in the condensation cloud on the upper surface of the aircraft. Further analysis of the data suggested that the RPO was a result of the interaction of the aircraft short period and first flexible bending mode of the aircraft with the oscillating shock. To better understand this RPO, an analysis effort was undertaken in which a viscous/inviscid interaction version of the CAP-TSD CAE code, known as CAP-TSDV¹⁹, was modified to include the short period dynamics and the active flight control system of the aircraft. Time simulations of two conditions resulting in RPO were analyzed using CAP-TSDV with mixed results.

Figure 11 shows the B-2 planform, with the CAP-TSDV model superimposed on it. The dashed line in the figure shows the actual planform and control surfaces, while the solid line shows the CAP-TSDV representation of these components. There are a number of restrictions to the modeling capability in CAP-TSDV that precluded modeling the actual vehicle planform and control surfaces. Thus the

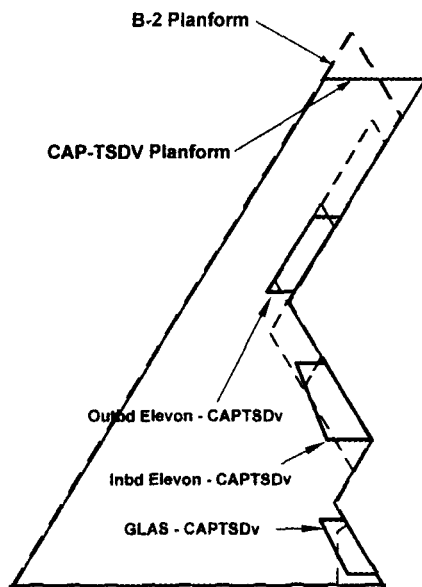


Figure 11. CAP-TSDV model and actual B-2 planform and control surfaces. (Reference 21)

control surface hinge lines and edges as well as the aircraft wing tip geometry can only be approximated by the CAP-TSDV methodology. In this analysis, only the control surfaces actively moving during the observed RPO response were modeled allowing the middle elevon and the outboard split drag rudders to be omitted from the model.

The first five elastic modes as well as the rigid body pitch and plunge modes were modeled in the CAP-TSDV analysis. A simplified pitch control augmentation Flight Control System (FCS) was also included in the CAP-TSDV model to actively deflect the control surfaces during the simulation. This allowed both open- and closed-loop simulations to be performed, and the impact of the control system on the RPO behavior to be assessed. Vertical acceleration and pitch rate responses computed by CAP-TSDV at the flight vehicle sensor locations were used as feedback sensor inputs for the FCS model. In addition, some of the nonlinear actuator characteristics of the flight vehicle were also modeled in the CAP-TSDV analysis.

CAP-TSDV time simulations were initiated using a converged, steady state, trimmed analysis of the aircraft at a specified flight condition. The inboard elevon was deflected using a control surface doublet command to perturb the vehicle, and the resulting pitch response was computed by CAP-TSDV.

Both open and closed-loop simulations were performed, and results for a heavy-weight, forward-CG configuration are shown in Figure 12. The open-

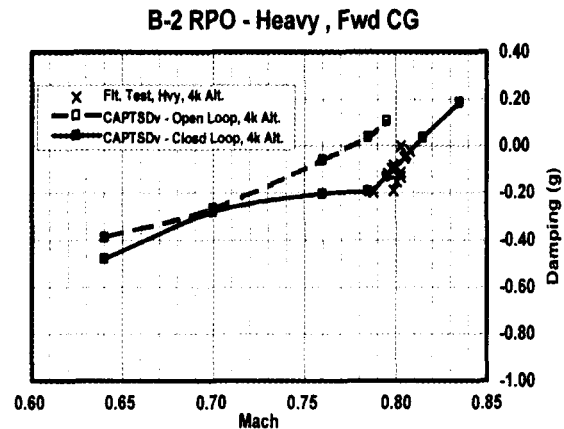


Figure 12. Computed and flight test B-2 RPO damping characteristics. (Reference 21)

loop simulation shows the vehicle to reach neutral stability (zero damping) at a lower Mach number than with the flight control system engaged. The closed-loop results closely match the flight test results at these conditions. The sharp break in the closed-loop damping characteristics has been assessed to be due to the formation of shock waves on the vehicle. The predicted frequency characteristics of the RPO, which are not shown here, also correlate with the flight test data at these conditions.

A second, lighter-weight configuration that exhibited the RPO phenomenon was also analyzed. CAP-TSDV did not predict the phenomenon as accurately as for the heavy-weight case. It over-predicted the severity of the RPO as compared to flight test, and also did not capture the fact that the RPO tended to stabilize as the Mach number was further increased. Several reasons for this poorer performance have been postulated, including CAP-TSDV's ability to accurately predict the streamwise and spanwise separated flow regions at these conditions, but further research is required to formulate hard conclusions.

RANS Analysis of Oscillating Flap and Spoiler Configurations

The CAP-TSDV analyses of the B-2 have demonstrated the utility of viscous/inviscid interaction methods in computing fully coupled aeroservoelastic problems of relatively severe complexity. However, these methods have known limitations, particularly when attempting to simulate moderately to severely separated and three-dimensional separated flows. The next step up in flow physics fidelity is to solve the Reynolds averaged Navier-Stokes (RANS) equations, and flow around deflected control surfaces is a prime candidate for application of this technology.

A number of studies have been performed modeling deflected control surfaces with higher-order aerodynamic methods²²⁻²⁸. References 22-25 represent a significant body of work investigating modeling and solution techniques for trailing edge control surfaces. In these studies, particular attention has been paid to the accurate modeling of the discontinuities at the spanwise edges of control surfaces. The ENSAERO Euler/Navier-Stokes CAE method²⁹ was used for these studies, which were confined primarily to low aspect ratio, high sweep, thin wings and wing-body configurations. The correlation with experimental data for these cases is, in general, very good, but transonic effects for these types of geometries are typically small compared to lower sweep wings with thicker wing sections.

Bartels and Schuster²⁶⁻²⁸ performed computations on the NASA Langley Benchmark Active Controls Technology (BACT) wing comparing two different RANS methods, CFL3Dv5.0³⁰ and ENS3DAE³¹. The BACT wing has a rectangular planform and a 12% thick symmetrical airfoil section. The planform and control surfaces for the wing are shown in Figure 13. The two methods were compared with each other and against experimentally measured unsteady pressures along the midchord of the aileron. The analyses were performed at Mach 0.77 with the aileron oscillating sinusoidally at 5 Hz. Figure 13(b) shows the real and imaginary pressure coefficient plotted versus percent chord along the wing section. The computations were performed on identical grids with the only differences in the calculations being in the formulation of the equations and the turbulence modeling. The ENS3DAE calculations were performed using a central finite difference method and the Baldwin-Lomax turbulence model, while the CFL3D calculations were performed using an upwind finite volume method and the Spalart-Allmaras turbulence model. For the most part, the two methods give similar results with differences in the peaks at the aileron hinge line and in the imaginary component of the pressure coefficient. The imaginary component of the pressure is very small compared to the real component for this case, and differences in the imaginary component plot are over exaggerated due to the fact that the vertical axis scale factor is five times that used for the real component plot.

CFL3D calculations of the wing with an oscillating spoiler have also been performed by Bartels³². The results of these calculations at Mach 0.77 with a mean spoiler deflection of 5°, and a spoiler oscillation of 4.5° at 9.56 Hz. are shown in Figure 14. The computation of an oscillating spoiler geometry and quantitative comparison with experimental data is

believed to be unique and represents the type of analysis that can be accurately performed using innovative modeling techniques.

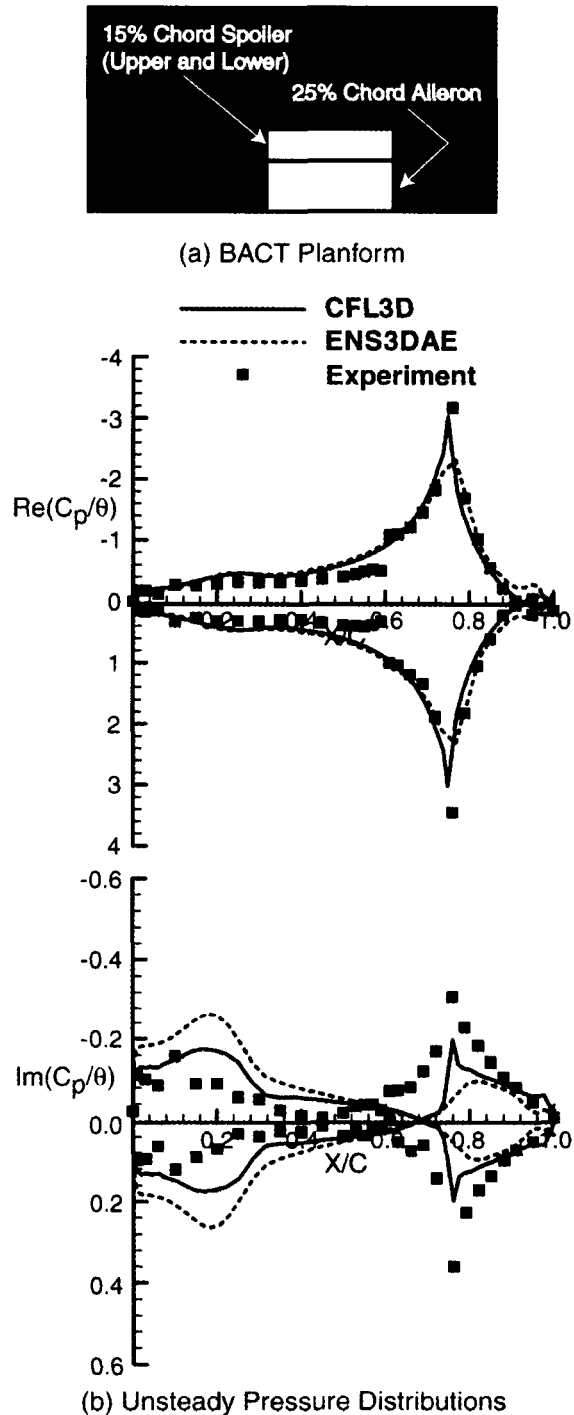


Figure 13. BACT wing planform and unsteady pressure distributions due to aileron oscillation, $M = 0.77$, $\alpha = 0.0^\circ$, $\delta_{Ail} = 0.0^\circ$, $\theta_{Ail} = 2.0^\circ$, $f_{Ail} = 5$ Hz. (Reference 27).

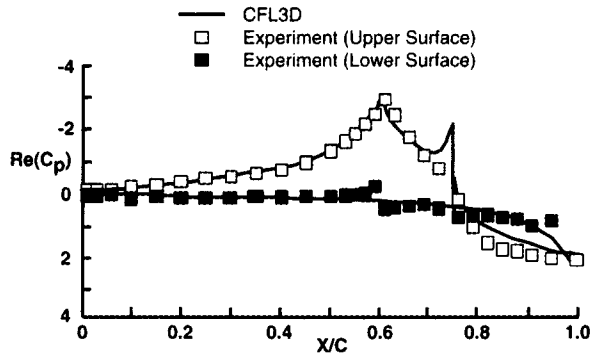


Figure 14. Real component of unsteady pressure for the BACT wing with an oscillating upper surface spoiler, $M = 0.77$, $\alpha = 0.0$, $\delta_s = 5.0^\circ$, $\theta_s = 4.5^\circ$, $f = 9.56$ Hz. (Reference 32).

Limit Cycle Oscillation Using Viscous/Inviscid Interaction Aerodynamics

Considerable progress has been demonstrated in the use of lower-order viscous/inviscid interaction methods to model separation onset and mildly separated flows, particularly those cases leading to Limit Cycle Oscillation (LCO).

The LCO phenomenon can be triggered by several mechanisms. Nonlinearities in the aerodynamics, structures, or the vehicle control system can result in the quenching of an instability, or in the case of the B-2, prevention of a convergent system from reaching a static steady-state. Aerodynamic nonlinearities are difficult to model and predict due to the complex flow interactions involved. Also, the nonlinearities producing the LCO often involve a transition in flow state, such as the appearance and disappearance of shock waves, vortices, and separated flow regions.

Coupling of Transonic Small Disturbance (TSD) potential flow methods, such as CAP-TSD, with interactive boundary layer schemes has proven to be effective in the prediction of LCO phenomena triggered by separation onset and shock-induced separated flow. The B-2 RPO example discussed earlier in this paper is a prime example of the use of this type of methodology to predict complex LCO problems.

Edwards³³ has presented a second example for a business jet wing operating at transonic conditions. This case is interesting because it is purely an aerodynamics/structural LCO triggered only by nonlinear aerodynamics. The mechanism involved in this LCO is one of shock-induced separation at conditions below the transonic flutter boundary. The LCO involves the excitation of the first bending

mode of the wing. Figure 15 summarizes the result of a CAP-TSDV analysis of the business jet wing at Mach 0.89 and dynamic pressure of 79 psf. In this figure, the vertical deflection of the wing tip is plotted as a function of time for two different initial displacements of the wing tip. The top figure shows that if the wing tip is displaced to a large deflection, the motion will decay to the experimental limit cycle amplitude. Likewise if the tip is initially displaced to a small deflection, the amplitude will grow until it reaches the LCO amplitude. This behavior is an important characteristic of the LCO phenomenon. The CAP-TSDV analysis captures a transient shock-induced separation on the outboard portion of the wing that is responsible for the LCO behavior. Further experiments on this wing³⁴ have verified this mechanism and identified a second transonic LCO phenomenon that involves the wing's first torsion mode.

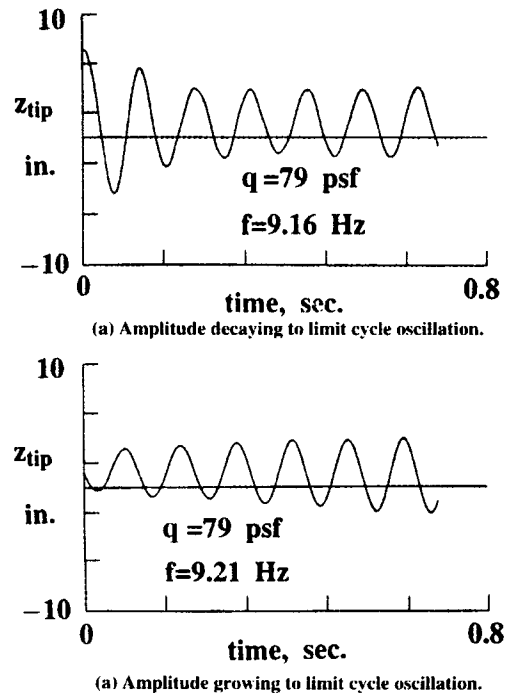


Figure 15. Computed business jet wing tip deflection time histories showing limit cycle oscillation, $M = 0.89$ (Reference 33).

The two LCO examples presented in this paper have demonstrated the utility of viscous/inviscid interaction methods for these types of predictions. However, the current methodology requires refinement and improvement in a number of areas.

At present, the boundary layer formulations included in the analyses are a simple strip implementation of the 2-D compressible integral boundary layer equations. The implementation of the viscous

equations is also only quasi-steady. Three-dimensional effects can be very important if not dominant on many modern configurations, and the two-dimensional implementation of the viscous modeling is certainly restrictive. The impact of the quasi-steady implementation of the equations has yet to be fully quantified.

On the inviscid side of the methodology, the TSD potential flow formulation of the equations limits the application of the method to flows with weak shocks and those without vortices. Higher-order inviscid formulations, such as the Euler equations, would relieve some of these restrictions.

The coupling of the methodologies, while well posed for steady flows, remains somewhat in question for unsteady flows. Addition of the viscous simulation using present techniques can have a destabilizing effect, and many times viscous computations cannot be performed, due to stability issues, in regions where similar inviscid computations can be performed.

Each of the above topic areas is ripe for further investigation by the research community.

Reduced Order Modeling (ROM) for Aeroelastic Applications

Finally, one cannot ignore the recent advances and contributions of Reduced Order Modeling (ROM) for aeroelastic and aeroservoelastic applications. ROM proposes to define methodology by which physically complex dynamic phenomena can be characterized and modeled at a reduced computational cost. In addition, important physical characteristics of the system can be extracted that often cannot be identified using traditional simulation techniques. The methodology formulates strategies for identification of linear and nonlinear kernels for a given aeroelastic system. These kernels are generated using a fixed number of numerical time simulations of the system response due to a generic input, such as a pulse. These kernels can then be superimposed, through convolution, to model the system response to an arbitrary input. This type of methodology especially benefits applications such as nonlinear control system design, where the burden of many nonlinear time simulations of the complete system for each control input can be reduced to just a few simulations of the complete system for a generic input followed by many simulations using the ROM.

Beran and Silva³⁵ and Dowell and Hall³⁶ provide excellent overviews of the ROM techniques under development today. A recent application by Silva and Bartels³⁷ has demonstrated the use of RANS simulation methodology to model the transonic

flutter of the AGARD 445.6 wing. Hong et al.³⁸ have also used this ROM technique to simulate the unsteady aeroelastic characteristics of more complex and realistic configurations. In these references, the effort required to perform a transonic flutter analysis of the wing using time simulation techniques is compared with the use of ROM.

The technique utilized in Reference 37 requires that an aeroelastic transient due to pulse inputs in each structural mode be computed to build the ROM. In general, each of these pulse response computations are less expensive than an aeroelastic transient since the pulse responses tend to return to a steady state in fewer cycles of motion than what is required to extract frequency and damping information from a typical aeroelastic transient. Once the pulse response for each mode has been computed, the fully coupled aeroelastic response can be computed for any dynamic pressure by superimposing the impulse response characteristics through convolution. The transients computed using the ROM are relatively inexpensive to compute.

For highly complex problems where a large number of structural modes are required, the computational cost of generating modal ROM responses will increase and may surpass the cost of standard simulations. However, a primary reason for generating aeroelastic ROM models is to develop insight into the nature of the computational responses as contrasted with traditional linear aeroelastic analyses. As shown in Reference 37, the comparison between CFD-based aeroelastic analyses and linear frequency-domain aeroelastic analyses can be easily performed using the CFD-based aeroelastic ROMs. In addition, methods are being developed that will enable the generation of modal-based ROMs using a single input, as opposed to an input per mode.

Thomas, et al.^{39,40} present a method whereby the order reduction more directly attacks the fluid solution, thus relieving the dependence of the ROM on the specific modal motions of the body. Their method, known as the Harmonic Balance technique, allows reduced order models of the fluid problem to be developed by a superposition of a series of harmonics. These reduced order fluid models can then be coupled to structural dynamics and control simulations to efficiently perform aeroelastic and aeroservoelastic analyses. In this case, the issue becomes how many harmonics to retain to obtain a sufficiently accurate aerodynamic analysis of the problem.

Further research and application of ROM techniques will relieve many of the issues discussed above, and this methodology certainly holds significant promise for future aeroelastic analysis.

CHALLENGES TO COMPUTATIONAL AEROELASTICITY

The previous sections have discussed the areas where CAE has been used to model problems of interest to both the aircraft development and design community as well as for aeroelastic research applications. However, there are a number of areas where CAE techniques fall well short of known analysis requirements. Some of these areas will be discussed here as the “challenge” to CAE.

Robust, Automated Linear Flutter Analysis for Design

As an analysis tool, linear flutter methods have certainly matured to the state where they are widely applied in the aerospace industry on a day-to-day basis. While great strides have been made in coupling these methodologies with mainline structural analysis tools used in the design environment, linear flutter analysis still requires a significant amount of user interaction to perform a given simulation. This lack of automation of the analysis itself has precluded its integration into the design optimization environment, and it continues to be exercised as a post-design analysis tool.

Part of this problem is due to the complexity of the flutter analysis itself, but a stagnation of algorithm development focused on automating the process is probably also to blame. Output from a typical p-k flutter analysis for a transport wing is shown in Figure 16. In contrast to the wing flutter analyses shown earlier in this paper, which consisted of 10 structural modes or less, this analysis contains 34 structural modes, plus six rigid body degrees of freedom. The figure plots modal damping versus airspeed with negative values of damping indicating aeroelastically stable motions and positive values indicating unstable motion. The critical point is when a given mode crosses the zero-damping axis, which defines the flutter boundary. The plot is very complicated with several modes, designated by the red letters, crossing the zero-damping axis.

To effectively incorporate flutter in the design optimization process, the data of an analysis similar to that shown in Figure 16 must be interrogated at each design condition to determine if a flutter constraint has been compromised. Simply tracking the modes in the above data is a formidable task, and while we have tools for this purpose, they are not infallible. For complicated systems as this, it is easy to lose track of modes, and inaccurately predict the critical flutter crossing.

It also is common for the flutter mechanism to change as the structural properties and even flight conditions change. Vehicles often have multiple

flutter modes simultaneously active for any given flight condition. The most critical mode is the one that occurs at the lowest airspeed because the vehicle will encounter it first. But relatively small changes in the vehicle structural properties and/or flight conditions can cause flutter modes to shift dramatically, making formerly benign flutter modes critical. This can be very confusing to an automated design process since vastly different structural properties may be important to the individual flutter modes.

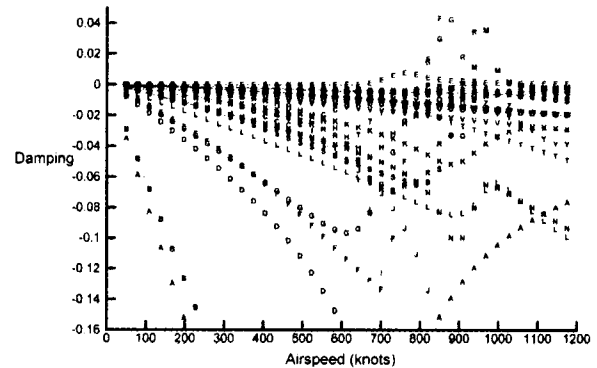


Figure 16. Typical flutter analysis results for a transport aircraft.

Further complicating the issue is the fact that some flutter crossings are very shallow as depicted by the mode labeled E in Figure 16. These shallow crossings can be physical flutter modes as is the case in so-called “hump” flutter modes, or they can be an artifact of the structural modeling. One common cause for these types of crossings is the presence of in-plane modes. For a lifting surface like a wing this would be a mode with deflection that is primarily in the plane of the wing, as opposed to one with deflection normal to the wing plane. Linear flutter analyses cannot accurately account for these types of motions and the simulation can predict non-physical flutter mechanisms. When this occurs, these in-plane modes are usually excluded from the flutter analysis to avoid the confusion caused by their presence. Aeroelasticians also often perform modal reduction to exclude modes that are not important to the flutter analysis and thus provide a clearer picture of the flutter characteristics of the vehicle. These types of operations are difficult to automate for use in a design environment.

Finally, the simple mathematics of the linear flutter problem can generate spurious roots to the equations that can flag false-positive results. These spurious roots are due to poor conditioning of the matrices as the problems become more complex and more modes are retained in the flutter analysis. Edwards and Wieseman⁴¹ discuss many of these issues when

describing the development of the Generalized Aeroelastic Analysis Method (GAAM). Automatically detecting and eliminating these roots from consideration is a must for incorporation of linear flutter methods in the automated design process.

In short, linear flutter analyses require a higher level of automation and further improvements in robust operation before they can be realistically incorporated in a multidisciplinary design/optimization environment. The computational requirements of these methods are well suited to today's computer resources, and efficiency is not a major issue preventing this assimilation. At present, the entire flutter analysis process requires too much user intervention and control to be effectively incorporated in the design environment.

Efficient Nonlinear Unsteady Aerodynamic Analysis

A significant deterrent to the widespread use of high-level CFD methods in aeroelastic and aeroservoelastic analysis is the computational efficiency of the methods. Significant effort has been devoted to the development and application of steady CFD, and this attention to the efficiency issues has paid off with the routine use of steady CFD, throughout the industry, as a mainstream aerodynamic analysis technique. Unfortunately unsteady aerodynamic analysis has tended to be neglected during this development period, and we are only now beginning to seriously assess the ability of many of the steady CFD codes to effectively handle unsteady problems.

In retrospect, some of the techniques used to improve the efficiency of steady CFD methods may not be amenable to the analysis of unsteady flows. For instance, it has long been known that the low frequency transients in a CFD simulation are a primary contributor to slow convergence rates. Significant efforts have been focused on rapidly eliminating these low frequency transients to improve convergence to a steady state. However, many aeroelastic and aeroservoelastic problems involve relatively low frequency phenomenon, and the techniques used to develop some of today's fastest steady CFD codes may make them inappropriate for unsteady analyses due to their low-frequency damping characteristics.

A second example illustrating this point is the widespread use of domain decomposition to perform parallel computations for steady CFD analyses. By breaking the computational grid into many sub-domains, or blocks, CFD computations about complex configurations involving millions of grid

points can be effectively spread across many computer processors. However, extending this technique to unsteady flows results in the introduction of time lags in the unsteady analysis along each of the arbitrary sub-domain boundaries. These lags force the user to use subiterations as the problem is broken into smaller blocks and spread across more processors. This has a profound impact on efficiency since the addition of just a single subiteration at best doubles the computer time required to solve the problem. Solution of the unsteady flow problem becomes dependent on the number of sub-domains, and the manner in which the global domain is subdivided.

New parallel processing algorithms for unsteady flows must be investigated to remove the dependence of the problem on the number of processors used to solve the equations. In other words, the solutions obtained for any given unsteady flow analysis should be identical for any number of processors used to solve the equations. This requires that implicit boundary conditions be employed at sub-domain boundaries when using domain decomposition, or new parallel strategies that operate at the numerical algorithm level must be developed.

Another limiting factor is the size of time step that can be taken by a given CFD code to perform an unsteady computation. Many techniques, including implicit formulations, are limited to small time steps to maintain stability. One method that has become popular among CFD developers is the incorporation of subiteration to help converge the nonlinear aerodynamic solution between time steps. Pulliam⁴² recommends this approach to improve the accuracy of diagonal implicit methods, and Jameson⁴³, Melson, et al.⁴⁴ and Rumsey et al.⁴⁵ describe methods incorporating a dual time-stepping technique and multigrid for both accuracy and efficiency improvement of traditional factored schemes.

One must be careful however when assessing these methods for efficiency since each subiteration within a time step is as costly or more costly than a single time step by conventional time-stepping algorithms. This issue is highlighted by Bartels and Schuster²⁷ using the previously discussed oscillating aileron case as an example. The results of their experience are shown in Table 1, which shows that the CFL3D aeroelastic method using subiteration could take a time step over 25 times larger than the ENS3DAE method without subiteration. However, the CFL3D calculation required 6 subiterations per time step, and the net gain in computational work was reduced to a factor of 4.3 over the ENS3DAE solution. Comparing this net gain in efficiency to the potential loss in accuracy for taking a significantly larger time

step, one can quickly see that there is a complex trade-off between accuracy and efficiency that must be weighed when employing subiteration.

Currently, unsteady computations can be an order-of-magnitude or more costly than a steady flow analysis. This cost has constrained most unsteady flow applications, beyond simple research demonstrations, to be performed using structured grid formulations, which are inherently more computationally efficient than unstructured grid methods. This restriction has a direct impact on the amount of human resources required to simulate a given problem, particularly for complex

Table 1. Impact of subiteration on efficiency of BACT oscillating aileron calculation (Reference 27).

BACT Oscillating Aileron Analysis	ENS3DAE	CFL3D
Time Steps per Cycle	3300	128
Subiterations	1	6
Computational Work per Cycle	3300	768
CPU Time per Cycle (Minutes)	175	35

configurations, and ultimately limits the acceptance of the methodology by potential users outside the CFD community. Both of these issues are discussed in subsequent sections. In short, there is significant margin for further development of efficient and accurate methods for the computation of unsteady nonlinear flows. As steady method development continues to mature, it is hoped that the resources and effort devoted to steady methods will be directed toward the development of new unsteady algorithms and strategies.

Robust Moving Grid Methodology

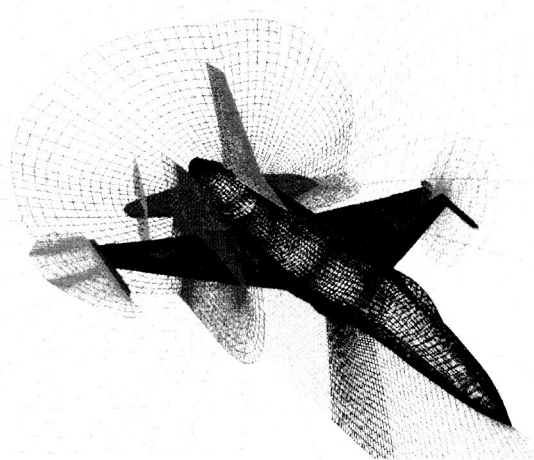
A key issue that separates the application of Euler and RANS aeroelastic methods from linear and even TSD potential flow aeroelastic schemes is the requirement of the former methods to physically move and deform the model and its surrounding grid. Linear methods eliminate the physical deformation of the vehicle from the problem by assuming small perturbation boundary conditions. TSD unsteady aerodynamics methods make a similar assumption. However, most Euler and RANS formulations employ the full surface boundary condition in their formulation, and the physical motion of the boundaries, as well as the grid surrounding the vehicle is captured directly in the equations of motion. This is the most accurate approach to

simulating the unsteady aerodynamics of the vehicle, but it introduces a major complication to the analysis. Efficiently moving what can amount to millions of grid points, thousands of times during an aeroelastic calculation is a daunting task in and of itself. The fact that the grids must also be moved in such a fashion as to not degrade grid quality or introduce crossed grids or negative cell volumes adds further complication.

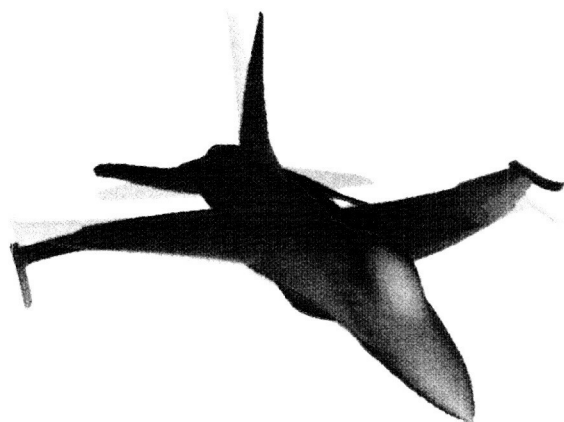
A significant body of research has been performed in the area of grid motion schemes for aeroelastic analysis. These range from simple algebraic shearing methods to those that model the vehicle and the surrounding grid as a physical field equation that can be coupled with the analysis. Schuster, et al.³¹ introduce a simple one-dimensional algebraic shearing technique that is very efficient and is suitable for structured grid topologies. This method is effective for many geometries of interest, particularly planar lifting surface and some control surface deflection²⁶ applications. However, as geometric and/or grid topology complexity increases, these simple methods begin to break down. Several researchers have extended the algebraic grid deformation approach to the use of transfinite interpolation (TFI) of the structural deformations⁴⁶⁻⁴⁸, which enable application to more complex block, structured grid topologies. Batina^{49,50} introduced a deforming mesh algorithm based on a spring analogy that was originally developed for triangular and tetrahedral unstructured grid applications, and was later extended to hexahedral cells for structured grid applications by Robinson, et al.⁵¹ Both the TFI approach and the basic spring analogy suffer from the similar character that grid skew can be exaggerated as the grid is deformed and in extreme cases, grid crossing can occur. To combat this problem, Farhat, et al.⁵² recommend the use of vertex-placed torsional springs to control the angle between grid element edges. Bartels⁵³ further addresses these issues by imposing more strict orthogonality rules on the grid deformation in the vicinity of the vehicle surface.

Each of the above methods requires some knowledge of the grid topology and/or connectivity between grid points. Recent grid deformation research appears to be moving toward the removal of this restriction. Chen and Hill⁵⁴ describe a technique that models the volume surrounding the vehicle with an elastic homogenous solid. In this case, each grid point surrounding the vehicle is associated with a specific location in the solid, while the vehicle surface lies on the boundary of the solid. As the vehicle deforms the elastic equations of motion are solved using a Boundary Element Method (BEM). Each point in the grid moves according to the elastic deformation of

the solid, therefore, no information concerning the structure, topology, or connectivity of the grid are required to define the grid deformation. Melville⁵⁵ describes a similar procedure that uses a distance relationship between the individual grid points and the vehicle surface to determine the grid deformation, again without knowledge of the grid topology or grid point connectivity. He has used this technique to perform an aeroelastic simulation of a complete F-16 configuration. The grid system and one of the structural modes associated with the analysis are shown in Figure 17. As can be seen, the geometry, the associated structured, multiblock grid, and the structural deformation for this analysis are all very complex. The fact that an aeroelastic simulation can be performed on a model of this complexity is a



(a) Complex Multiblock Grid System



(a) Complex Structural Deformation

Figure 17. Grid and structural deformation associated with the aeroelastic analysis of an F-16 aircraft (Reference 55).

testament to the grid motion scheme employed in the analysis.

Though significant progress has been realized in the development of grid deformation schemes, no single technique has been identified as having significant benefits over the others. It appears the preprocessing approaches to the problem are gaining favor since it allows the user to assess the suitability of the grid, ahead of time, for worst-case deformations. However, there is still significant opportunity to make advances in this area of research.

Complex Configuration Aeroelasticity

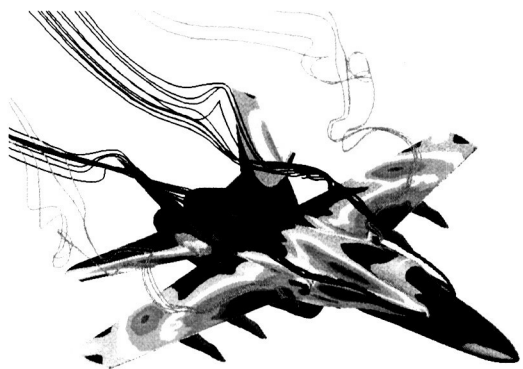
Many linear and nonlinear aeroelastic phenomena are the result of subtle structural and aerodynamic interactions between aircraft components. Engine/nacelle/pylon, wing store/pylon, strakes, chines, vortex generators, and fences are among the long list of components that can have a dramatic impact on both the steady and unsteady character of the vehicle aerodynamics and structural dynamics. It is often imperative to accurately and efficiently model these details when performing some aeroelastic analyses.

The importance of geometric details to the aerodynamic and aeroelastic performance of air vehicles is illustrated in Figure 18. Sheta and Huttzell⁵⁶ have numerically investigated the buffeting of the F-18 vertical tails due to the leading edge extension (LEX) vortices. The effects of adding LEX fences to the aircraft are clearly observed in the figure. In this 35° angle of attack calculation, the LEX vortex pattern is significantly altered through addition of the fences. This pattern has a direct impact on the dynamic loads experienced on the vertical tails of this aircraft. Thus this relatively small geometric detail has a major impact on the aeroelastic performance of the F-18 and other twin-vertical-tail fighters.

A second example is the Limit Cycle Oscillation (LCO) experienced on the F-16⁷. This nonlinear aeroelastic phenomenon manifests itself only for certain under-wing store configurations and flight conditions. It was not discovered prior to flight-testing of the aircraft. To date, this phenomenon continues to be the subject of significant debate throughout the aeroelastic community, and potential causes ranging from complex, unsteady transonic flow interactions to structural nonlinearities have been offered as the root cause for the LCO. As previously discussed, researchers have attempted to use modified linear methods to address this problem. Unfortunately we still do not possess high-order aeroelastic methods capable of accurately simulating



(a) LEX Fences Off



(b) LEX Fences On

Figure 18. Effect of Leading Edge Extension (LEX) fences on the vortex flow patterns on an F-18 aircraft.

the unsteady transonic flow about the highly complex store geometries of the F-16.

As these types of details are added to the simulation, the issues of the previous two sections become enabling to the aeroelastic analysis, particularly for high-order methods. However, just the modeling requirements associated with these configuration details can be significant even for steady flow problems. For this reason, the use of unstructured grids has become popular for many steady computational aerodynamics simulations on complex configurations. The computational resources required to perform unstructured grid computations are generally higher than those required for structured grid, but the time and human resources required to model complex configurations using unstructured grids is much smaller than for structured grids.

Unfortunately, the extension of unstructured grid technology to unsteady flows has not been thoroughly investigated, and further research in this area is required. Batina⁵⁷, and Rausch and Batina⁵⁸ have applied an unstructured grid Euler analysis

method to aeroelastic problems on complex configurations, and this work is most noted for the development of the spring analogy for grid deformation and their investigations into adaptive grid techniques for unsteady flows. Farhat, et al.⁵⁹ use a similar method to perform aeroelastic analysis on an F-16 configuration. Viscous computations using unstructured grids are becoming more commonplace for steady flows, but unfortunately their extension to unsteady flows and aeroelastic problems has not yet been realized.

Non-Expert User Environment

Perhaps the most daunting challenge faced by developers of future aeroelastic analysis and design methods is the formulation of tools that can be employed by engineers who are not experts in the individual disciplines that form the methods. Aeroelasticity has a significant impact on the performance of modern air vehicles, and incorporating aeroelastic considerations early in the design process can help developers avoid design surprises in the latter stages of the aircraft development, where fixes to the problem can be very costly both financially and to vehicle performance. If these methods are integrated into the preliminary design process, engineers that are experts in fields other than CFD, finite element structural modeling, flight controls, or even aeroelasticity will use them. This will require that the methods be significantly more robust and automated than current methods, particularly for the higher-order formulations.

The developers of higher-order methods must aggressively address this situation if these tools are to be used in a fashion even similar to present linear methods. Aeroelastic analysis of flight vehicles is not optional, and organizations will take the path of least resistance to meet their aeroelastic analysis needs. At present, high-order aeroelastic methods require a significant investment in time, human, and computer resources. Until these investments are reduced, high-order aeroelastic methods will continue to be viewed as optional and their application will be intermittent at best. Even though the cost of aeroelastic wind-tunnel and flight testing is very high, maintaining a specialized staff simply to employ high-order aeroelastic methods is higher. Aircraft manufactures will continue to maintain the status quo in regard to aeroelastic analysis until these methods become more cost-effective.

GLIMPSES OF THE FUTURE OF CAE

Computational Aeroelasticity continues to play a critical role in the development of modern air vehicles. The current suite of linear aeroelastic, aeroservoelastic, and gust response methodologies

serves as the mainstay for aeroelastic analysis and they form a solid base on which to build future developments. Unfortunately, modern aircraft systems continually uncover aeroelastic issues that cannot be effectively predicted by these methods, and as a result, costly aeroelastic wind-tunnel and flight tests must be conducted to investigate and rectify these problems. This situation is envisioned to worsen as new concepts, such as morphing, continuous moldline controls, etc., call for vehicles with higher degrees of structural flexibility.

Many of today's analyses investigate only the aeroelastic stability of the vehicle, where small aeroelastic perturbations can be assumed and the impact of wing thickness and camber and even static aeroelastic deformation can be neglected. These characteristics will not be negligible on many future vehicles, and heretofore accepted and/or calibrated errors from linear aeroelastic analysis will no longer be acceptable.

Therefore it is imperative that higher-order aeroelastic methods continue to be developed and refined. Many of today's problems already require the inclusion of transonic and separated flow effects, detailed structural modeling, and provisions for including structural nonlinearities. Future applications will likely require that temperature effects and chemical reactions be included in the simulations. It is our opinion that methods should continue to be developed on three levels of complexity:

- 1) Linear Methods
- 2) Moderate Fidelity Methods (including viscous/inviscid interaction techniques, Reduced Order Modeling, etc.)
- 3) High-fidelity methods (Reynolds Averaged Navier-Stokes Aerodynamics, structured and unstructured grid methods, nonlinear finite element modeling, etc.)

During this development, consideration must be given to how the methods can be effectively employed in a design environment, not just as a post-design analysis tool. They should also be developed with the specific objective that they be readily integrated into existing aeroelastic analysis frameworks. Finally, and most importantly, the new methods must be sufficiently general in application, robust and efficient in operation, and simple in implementation to make them a viable tool for general use in the aerospace industry.

REFERENCES

1. Theodorsen, T., "General Theory of Aerodynamic Instability and the Mechanism of Flutter," NACA Report Number 496, National Advisory Committee for Aeronautics, May 1934.
2. Giesing, J. P., Kalman, T., and Rodden, W. P., "Subsonic Unsteady Aerodynamics for General Configurations; Part II, Volume II – Computer Program N5KA," Air Force Flight Dynamics Laboratory Report No. AFFDL-TR-71-5, Part II, Vol. II, 1972.
3. Liu, D. D., James, D. K., Chen, P. C., and Pototzky, A. S., "Further Studies of Harmonic Gradient Method for Supersonic Aeroelastic Applications," *Journal of Aircraft*, Vol. 28, pp. 598-605, September 1991.
4. Harder, R. L. and Desmaris, R. N., "Interpolation Using Surface Splines," *Journal of Aircraft*, Vol. 9, pp.189-191, 1972.
5. Chen, P. C., Sulaeman, E., Liu, D. D., and Denegri, C. M. "Influence of External Store Aerodynamics on Flutter/LCO of a Fighter Aircraft," AIAA Paper AIAA-2002-1410, April 2002.
6. "ZAERO: An Engineer's Toolkit for Aeroelastic Solutions, Theoretical Manual, Version 4.3," ZONA Technology, Inc., Scottsdale, AZ, info@zonatech.com, www.zonatech.com, Aug. 2000.
7. Denegri Jr., C. M., "Limit Cycle Oscillation Flight Test Results of a Fighter with External Stores," *Journal of Aircraft*, Vol. 37, No. 5, Sep.-Oct. 2000.
8. Chen, P.C., "Damping Perturbation Method for Flutter Solution: The g-Method", *AIAA Journal*, Vol. 38, No. 9, Sept 2000, pp. 1519-1524.
9. Karpel, M., Moulin, B., Chen, P.C., "Extension of the g-Method Flutter Solution to Aeroservoelastic Stability Analysis", AIAA Paper AIAA-2003-1512, April 2003.
10. Rogers, K. L., "Airplane Math Modeling Methods for Active Control Design" Structural Aspects of Active Control, Design, *Structural Aspects of Active Controls*, AGARD-CP-228, Aug. 1977, pp 4-1 to 4-11.
11. Karpel, A., "Extension to the Minimum-State Aeroelastic Modeling Method," *AIAA Journal*, Vol.29, No.11, 1991, pp.2007-2009.

12. Nam, C., Chen, P.C., Liu, D.D., Chattopadhyay, A., "ASTROS* with Smart Structures and ASE Modules: Application to Flutter Suppression and Gust-Load Alleviation," AIAA Paper AIAA-2000-1365, April 2000.
13. Johnson, E.H., and Venkayya, V.B., "Automated Structural Optimization System (ASTROS), Theoretical Manual," AFWAL-TR-88-3028, Vol. 1, Dec. 1988.
14. Chen, P.C., Liu, D.D., Sarhaddi, D., Striz, A.G., Neill, D.J. and Karpel, M., "Enhancement of the Aeroservoelastic Capability in ASTROS," STTR Phase I Final Report, WL-TR-96-3119, Sep. 1996.
15. Chen, P.C., Jha, R., Sarhaddi, D., Liu, D.D., Griffin, K. and Yurkovich, R., "A Variable Stiffness Spar (VSS) Approach for Aircraft Maneuver Enhancement Using ASTROS," AIAA Paper AIAA-99-1471, July 1999.
16. Lee-Rausch, E. M. and Batina, J. T., "Wing Flutter Computations Using an Aerodynamic Model Based on the Navier-Stokes Equations," *Journal of Aircraft*, Vol. 33, No. 6, November-December 1996, pp. 1139 – 1147.
17. Lee-Rausch, E. M. and Batina, J. T., "Wing Flutter Boundary Prediction Using Unsteady Euler Method," *Journal of Aircraft*, Vol. 2, No. 2, 1995, pp.416-422.
18. Gibbons, M. D., "Aeroelastic Calculations Using CFD for a Typical Business Jet Model," NASA Contractor Report 4753, September 1996.
19. Edwards, J. W., "Transonic Shock Oscillations and Wing Flutter Calculated with an Interactive Boundary Layer Coupling Method," EUROMECH-Colloquim 349, "Simulation of Fluid-Structures Interaction in Aeronautics," Goettingen, Germany, September 16-18, 1996.
20. Batina, J. T., Seidel, D. A., Bland, S. R., and Bennett, R. M., "Unsteady Transonic Flow Calculations for Realistic Aircraft Configurations," NASA TM 89120, March 1987.
21. Dreim, D. R., Jacobson, S. B., and Britt, R. T., "Simulation of Non-Linear Transonic Aeroelastic Behavior on the B-2," NASA/CP-1999-209136, Proceedings of the CEAS/AIAA/ICASE/NASA Langley International Forum on Aeroelasticity and Structural Dynamics 1999, June 1999, pp. 511 – 521.
22. Obayashi, S. and Guruswamy, G., "Navier-Stokes Computations for Oscillating Control Surfaces," AIAA Paper AIAA-92-4431, August 1992.
23. Klopfer, G. H. and Obayashi, S., "Virtual Zone Navier-Stokes Computations for Oscillating Control Surfaces," AIAA Paper AIAA-93-3363, July 1993.
24. Obayashi, S., Chiu, I-T, and Guruswamy, G. P., "Navier-Stokes Computations on Full-Span Wing-Body Configuration with Oscillating Control Surfaces," AIAA Paper AIAA-93-3687, August 1993.
25. Byun, C. and Guruswamy, G. P., "Aeroelastic Computations on Wing-Body-Control Configurations on Parallel Computers," AIAA Paper AIAA-96-1389.
26. Schuster, D. M., Beran, P. S. and Huttshell, L. J., "Application of the ENS3DAE Euler/Navier-Stokes Aeroelastic Method," AGARD-R-822, Paper 3, March 1998.
27. Bartels, R. E. and Schuster, D. M., "Comparison of Two Navier-Stokes Methods with Benchmark Active Controls Technology Experiments," *Journal of Guidance, Control and Dynamics*, Vol. 23, No. 6, December 2000, pp. 1094 – 1099.
28. Schuster, D. M., and Bartels, R. E., "Benchmark Active Controls Technology (BACT) Wing CFD Results," RTO-TR-26, *Verification and Validation Data for Computational Unsteady Aerodynamics*, October 2000, pp. 225-238.
29. Guruswamy, G. P., "Unsteady Aerodynamic and Aeroelastic Calculations for Wings Using Euler Equations," *AIAA Journal*, Volume 28, March 1990, pp. 461-469.
30. Krist, S. L., Biedron, R. T., and Rumsey, C. L., "CFL3D User's Manual (Version 5.0)," NASA/TM-1998-208444, June 1998
31. Schuster, D. M., Vadyak, J., and Atta, E., "Static Aeroelastic Analysis of Fighter Aircraft Using a Three-Dimensional Navier-Stokes Algorithm," *Journal of Aircraft*, Volume 27, Number 9, September 1990, pp. 820-825.
32. Schuster, D. M., Scott, R. C., Bartels, R. E., Edwards, J. W., and Bennett, R. M., "A Sample of NASA Langley Unsteady Pressure Experiments for Computational Code Evaluation," AIAA Paper AIAA-2000-2602, June 2000.

33. Edwards, J. W., "Calculated Viscous and Scale Effects on Transonic Aeroelasticity," AGARD-R-822, Paper 1, March 1998.
34. Edwards, J. W., Schuster, D. M., Spain, C. V., Keller, D. F., and Moses, R. W., "MAVRIC Flutter Model Transonic Limit Cycle Oscillation Test," AIAA Paper AIAA-2001-1291, April 2001.
35. Beran, P. and Silva, W., "Reduced-Order Modeling: New Approaches for Computational Physics," AIAA Paper AIAA-2001-0853, January 2001.
36. Dowell, E.H. and Hall, K.C., "Modeling of Fluid-Structure Interaction," Annual Review of Fluid Mechanics, 33:445-90, 2001.
37. Silva, W. A. and Bartels, R. E., "Development of Reduced-Order Models for Aeroelastic Analysis and Flutter Prediction Using the CFL3Dv6.0 Code," AIAA Paper AIAA-2002-1596, April 2002.
38. Hong, M. S., Kuruvila, G, Bhatia, K. G., SenGupta, G., and Kim, T., "Evaluation of CFL3D for Unsteady Pressure and Flutter Predictions," AIAA Paper AIAA-2003-1923, April 2003.
39. Thomas, J.P., Dowell, E.H. and Hall, K.C., "Three-Dimensional Transonic Aeroelasticity Using Proper Orthogonal Decomposition Based Reduced Order Models," AIAA Paper AIAA-2001-1526, April 2001.
40. Thomas, J.P., Dowell, E.H. and Hall, K.C., "Modeling Viscous Transonic Limit Cycle Oscillation Behavior Using a Harmonic Balance Approach," AIAA Paper AIAA-2002-1414, April 2002.
41. Edwards, J. W. and Wieseman, C. D., "Flutter and Divergence Analysis Using the Generalized Aeroelastic Analysis Method," AIAA Paper AIAA-2003-1488, April 2003.
42. Pulliam, T., "Time Accuracy and the Use of Implicit Methods," AIAA Paper AIAA-93-3360, 1993.
43. Jameson, A., "Time Dependent Calculations Using Multigrid, with Applications to Unsteady Flows Past Airfoils and Wings," AIAA Paper AIAA-91-1596, 1991.
44. Melson, N., Sanetrik, M., and Atkins, H., "time-Accurate Navier-Stokes Calculations with Multigrid Acceleration," NASA-CP-3224, Part 2, 1993, pp.423-437.
45. Rumsey, C. L., Sanetrik, M. D., Biedron, R. T., Melson, N. D., and Parlette, E. B., "Efficiency and Accuracy of Time-Accurate Turbulent Navier-Stokes Computations," *Computers and Fluids*, Vol. 25, No. 2, 1996, pp.217-236.
46. Jones, W. T., and Samareh-Abolhassani, J., "A Grid Generation System for Multi-Disciplinary Design Optimization," AIAA Paper 95-1689-CP, June 1995.
47. Reuther, J., Jameson, J., Farmer, J., Martinelli, L., and Saunders, D., "Aerodynamic Shape Optimization of Complex Aircraft Configurations via an Adjoint Formulation," AIAA Paper 96-0094, January 1996.
48. Hartwich, P. M. and Agrawal, S., "Method for Perturbing Multiblock Patched Grids in Aeroelastic and Design Optimization Applications," AIAA Paper 97-2038, June 1997.
49. Batina, J., "Unsteady Euler Airfoil Solutions Using Unstructured Dynamic Meshes," AIAA Paper 89-0115, January 1989.
50. Batina, J. T., "Unsteady Euler Algorithm With Unstructured Dynamic Mesh for Complex-Aircraft Aeroelastic Analysis," AIAA Paper No. 89-1189, April 1989.
51. Robinson, B. A., Batina, J. T., and Yang, H. T., "Aeroelastic Analysis of Wings Using the Euler Equations with a Deforming Mesh," *Journal of Aircraft*, Volume 28, November 1991, pp. 778-788.
52. Farhat, C., Degand, C., Koobus, B., and Lesoinne, M., "An Improved Method of Spring Analogy for Dynamic Unstructured Fluid Meshes," AIAA Paper 98-2070, April 1998.
53. Bartels, R. E., "An Elasticity-Based Mesh Scheme Applied to the Computation of Unsteady Three-Dimensional Spoiler and Aeroelastic Problems," AIAA Paper 99-3301-CP, June 1999.
54. Chen, P. C., and Hill, L. R., "A Three-Dimensional Boundary Element Method for CFD/CSD Grid Interfacing," AIAA Paper 99-1213, August 1999.
55. Melville, R., "Nonlinear Mechanisms of Aeroelastic Instability for the F-16," AIAA Paper 2002-0871, January 2002.
56. Sheta, E. F. and Huttshell, L. J., "Numerical Analysis of F/A-18 Vertical Tail Buffeting," AIAA Paper AIAA-2001-1664, April 2001.

57. Batina, J. T., "Unsteady Euler Algorithm with unstructured Dynamic Mesh for Complex-Aircraft Aeroelastic Analysis," AIAA Paper AIAA-89-1189, April 1989.
58. Rausch, R. D. and Batina, J. T., "Three-Dimensional Time-Marching Aeroelastic Analyses Using an Unstructured-Grid Euler Method," AIAA Journal, Volume 31, No. 9, September 1993, pp. 1626-1633.
59. Farhat, C., Geuzaine, P., Brown, G., and Harris, C., "Nonlinear Flutter Analysis of an F-16 in Stabilized, Accelerated, and Increased Angle of Attack Flight Conditions," AIAA Paper, AIAA-2002-1490, April 2002.